EFFECT OF INTERFACE MICROSTRUCTURE ON THE MECHANICAL PROPERTIES OF Pb-FREE HYBRID MICROCIRCUIT SOLDER JOINTS

Cynthia L. Hernandez, Paul T. Vianco, Jerome A. Rejent
Sandia National Laboratories
Albuquerque, NM

ABSTRACT

Although Sn-Pb eutectic alloy is widely used as a joining material in the electronics industry, it has well documented environmental and toxicity issues. Sandia National Laboratories is developing alternative solder materials to replace traditional Pb-containing alloys. The alloys are based on the Sn-Ag, Sn-Ag-Bi and Sn-Ag-Bi-Au systems. Prototype hybrid microcircuit (HMC) test vehicles have been developed to evaluate these Pb-free solders, using Au-Pt-Pd thick film metallization. Populated test vehicles with surface mount devices have been designed and fabricated to evaluate the reliability of surface mount solder joints. The test components consist of a variety of dummy chip capacitors and leadless ceramic chip carriers (LCCC's). Intermetallic compound (IMC) layer reaction products that form at the solder/substrate interface have been characterized and their respective growth kinetics quantified. Thicker IMC layers pose a potential reliability problem with solder joint integrity. Since the IMC layer is brittle, the likelihood of mechanical failure of a joint in service is increased. The effect of microstructure and the response of these different materials to wetting, aging and mechanical testing was also investigated. Solid-state reaction data for intermetallic formation and mechanical properties of the solder joints are reported.*

Key Words: Pb-free solders, mechanical properties, solder microstructure, intermetallic compound growth

INTRODUCTION

Soldering is still the predominant technique used by the electronics industry for joining active and passive components. Solder joints were initially designed to be simple electrical interconnections in electronic packages. However, as technology advanced, electrical component size decreased, and the number of input/output terminations increased. To accommodate these changes, the numbers of solder joints per package increased while joint dimensions decreased. As technology continued to advance, the solder joint was expected to be both an electrical and mechanical connector. Surface mount technology (SMT) has, therefore, become increasingly important because of benefits, such as reduced size, increased reliability and increased speed due to greater packing density[1].

The most commonly used solders are eutectic or near eutectic Sn-Pb alloys. While they exhibit excellent wetting behavior at low temperatures, they also have well documented toxicity issues. New soldering materials and processes have been developed over the years to address environmental concerns. Ground water contamination by discarded electronic assemblies with Pb-bearing solders is of particular importance[2]. Several Pb-free solders have been developed over the years to address these concerns. New Pb-free alloys must meet the requirement of both a compatible melting temperature and low toxicity while maintaining good mechanical properties. This reduces the number of metals that can be considered as possible alternatives[3]. In general, Sn, with its desirable physical properties, is alloyed with other metals to produce acceptable materials. These include Sb, Bi, Au, Cu, Ga, In, Ag and Zn. Each metal has its own specific advantages and disadvantages when used as a constituent in a solder composition. In addition, the limited solubility of a specific metal within the Sn matrix can affect performance of the solder alloy[4].

Surface mount technology has been used to attach electronic components to ceramic substrates in the hybrid microelectronics industry. Thick film pastes or "inks" have a critical role in hybrid microcircuit (HMC) technology, as they form the conductive features and device attachment pads on the ceramic substrates. Traditionally, noble metals such as silver or gold have formed the basis of the conductive component of the thick film inks because of their stability in the presence of the glassing agent, as well as their limited oxidation in the air firing process[5]. Although pure Ag and Au are readily wetted by eutectic Sn-Pb solder, both metals are prone to significant dissolution or leaching by the molten solders during processing. A significant loss of thick film conductor increases the likelihood that the mechanical integrity of the solder joint will deteriorate. Two other metals, Pt and Pd, have properties which favor their use as thick film conductor materials, as well. In particular, they are considerably less susceptible to molten solder dissolution. Optimal thick film properties can, therefore, be realized by combining Ag, Au, Pt and Pd to benefit from the attributes of the individual components[6].

When molten eutectic Sn-Pb solder wets a substrate, reaction products known as intermetallics form at the solder/substrate interface. The thickness of the interfacial reaction layer increases rapidly during soldering and continues to grow through solid state diffusion after the joint has solidified[7]. While the presence of an intermetallic layer is evidence of a sound metallurgical bond, the resulting

* Sandia is a multiprogram laboratory operated by Sandia Corporation, a Lockheed Martin Company, for the United States Department of Energy under Contract DE-AC04-94AL85000.

DISCLAIMER

thickness of this layer is of particular importance to the integrity of a joint and, thus, to the reliability of the electronic device[8]. It is important to understand the time-temperature kinetics of intermetallic compound (IMC) layer growth to predict layer development as a function of thermal aging[9]. Excessive growth of the layer can cause the metallization and solder, to be consumed in the process. Loss of the thick film to IMC formation in the solid-state can jeopardize joint integrity. Consumption of the solderable metallization in the liquid state can result in dewetting of the solder.

EXPERIMENTAL

Several potential Pb-free solders were considered during the initial phases of the evaluation. Wetting behavior of Pb-free solders was determined by area-of-spread experiments on Au-Pt-Pd thick film. Flux residue corrosion behavior was characterized by temperature-humidity aging. Some alloys were eliminated from subsequent evaluation after baseline wetting and corrosion testing. This paper discusses the IMC growth kinetics and mechanical properties of the three best Pb-free alloys: Sn-Ag, Sn-Ag-Bi and Sn-Ag-Bi-Au. These were compared to the well known properties of eutectic Sn-Pb solder.

The solder compositions (expressed as wt.%) used in this study included the commercially available pastes, Sn63-Pb37 and Sn96.5-Ag3.5. The other two alloys have the composition Sn91.84-Ag3.33-Bi4.83 and Sn86.85-Ag3.15-Bi5.0-Au5.0 and were developed at Sandia National Laboratories. A differential scanning calorimeter (DSC) determined the onset temperature to be 212°C[2] for Sn-Ag-Bi and 195°C for the Sn-Ag-Bi-Au alloy.

Solid state aging experiments examined the long-term isothermal growth kinetics of the intermetallic compound layer that formed between the different solder alloys and the Au-Pt-Pd thick film. Solder bumps were formed on thick film pads and processed through a tabletop reflow machine. Each alloy was then heat treated to a set of aging conditions. The aging temperatures were 55°C, 70°C, 85°C, 100°C, 135°C, and 170°C. The aging times ranged from 10 hrs. to 5000 hrs.

The aged samples were metallographically cross-sectioned, mounted in cold setting epoxy, polished and examined for microstructural changes. It is necessary to clearly describe the manner in which the intermetallic compound layer thickness measurements were taken. Shown in Fig. 1 is an SEM/backscattered emission micrograph of an Sn-Pb cross section at the interface of the thick film layer and the solder field, from a sample aged at 85°C for 2000 hrs. Unlike the uniformly continuous intermetallic compound interfaces that are observed between Sn63-Pb37 solder and wrought metal substrates, such as Cu and Ni, a discontinuous intermetallic layer formed at the solder/thick film interface. Penetration of solder into the pores of the thick film cause a multi-directional growth of the IMC layer. In such regions, one-dimensional layer growth is not a valid assumption.

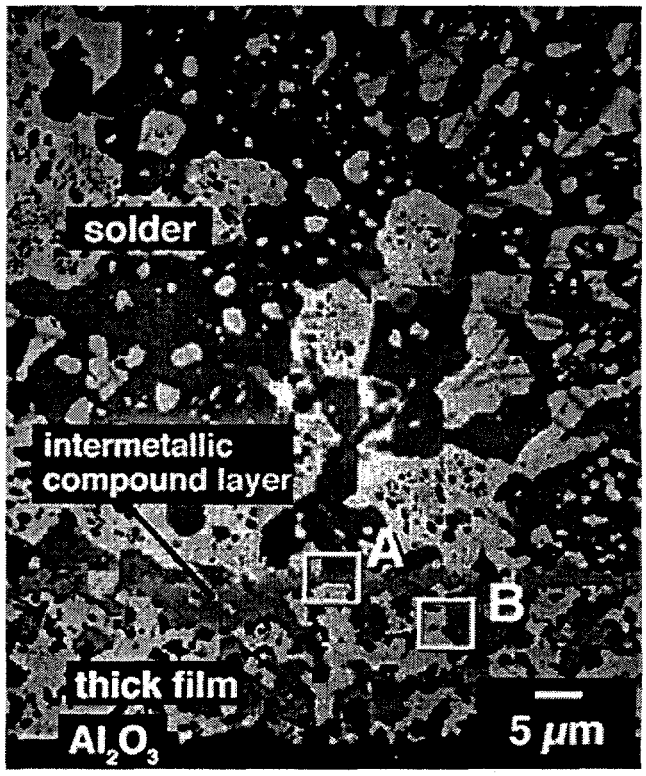

Figure 1. SEM/backscattered emission micrograph of the interface between Sn63-Pb37 solder and the Au-Pt-Pd thick film after aging at 85°C for 2000 hrs. Intermetallic compound layer thickness measurements were made at locations similar to "A". Locations such as "B" would not provide valid results.

Therefore, the following measurement technique was used. Those positions marking the furthest extent of the thick film into the solder were noted. Location "A" in Fig. 1 would represent such a case. On the other hand, at the "B" location inside a pore, intermetallic growth took place in all three directions. It was presumed that, at locations such as "A", truly one-dimensional growth took place in which the IMC layer grew normal to the interface. Because of this, IMC layer thickness measurements were taken only at locations represented by "A". Ten thickness measurements were taken directly from each micrograph. The data for each aging time and temperature is described by the mean thickness value plus or minus one standard deviation.

The next step in the evaluation was to determine the relative shear strength of the alloys. A ring-and-plug test methodology was developed for this purpose. The dimensions of the individual ring and plug pieces are shown in Fig. 2.

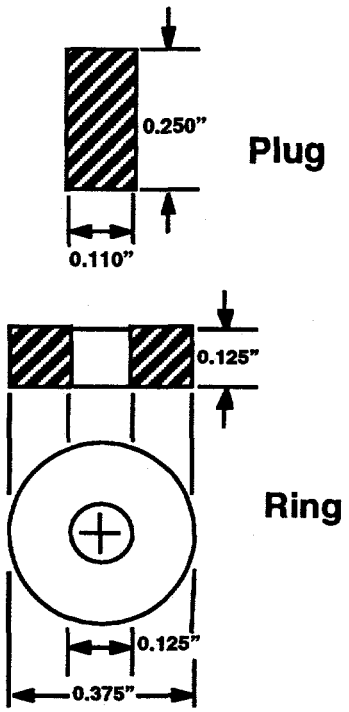

Figure 2. Ring-and-Plug test specimen geometry.

Oxygen-free high conductivity (OFHC) copper was used for the ring and plug structures. The inner diameter of the ring and the outer diameter of the plug produce a nominal solder joint gap of 0.0075 in. The sample preparation/assembly process is as follows: The ring and plug of each specimen was degreased in a solvent, etched in a 50% HCl:50% DI water solution, rinsed and dried. Each part was then coated with an RMA flux. An annular preform of each solder alloy was placed at the juncture between the ring and plug. The entire assembly was placed on a hot plate, set at a temperature of 300°C. It remained on the hot plate for a period of 20 sec. past the point at which the solder preform initially melted. The specimens were then removed from the hot plate, cooled on a chill block, and cleaned of flux residues.

Mechanical testing of the sample was performed by pushing the plug through the ring. The specimens were secured into a specially designed fixture. The fixture was then placed into a load frame. The maximum recorded load was used to designate the strength of the joint. The crosshead speed was 10 mm/min. The strength data is represented by the mean ± one standard deviation of all the measurements. This test data is shown in Table 1. The mechanical strengths of each of the Pb-free alloys are considerably higher than Sn-Pb.

Table 1. Shear Data for Ring-and-Plug Test Specimens

Solder	Load (lbs.)	Stress (psi)
Sn-Pb	269 ± 11	5840 ± 240
Sn-Ag	367 ± 24	7970 ± 530
Sn-Ag-Bi	540 ± 80	11800 ± 1700
Sn-Ag-Bi-Au	560 ± 15	12170 ± 330

Area = 0.046 in^2

The above solders demonstrated acceptable wetting, shear strengths and aging properties and were chosen to fabricate a prototype test vehicle. The hybrid microcircuit test vehicle (HMCTV) used in this study was a 96% alumina substrate with a Au76-Pt21-Pd3 (wt. %) thick film metallization. It measures 3.40" long x 2.50" wide x 0.040" thick. The Au-Pt-Pd film was double printed to a minimum thickness of 23μm in a repeated "print-dry-fire" procedure. In the double print process, the first ink deposit is screen printed onto the alumina substrate; the deposits are allowed to dry under conditions of 150°C, 10-15 min. in dry nitrogen. The substrate is fired at 825°C for 10 min. The second printing of ink is then applied to the substrate, allowed to dry and fired again at 825° for 10 min. The glass agents are a mixture of bismuth oxide, silicon oxide, lead oxide and calcium oxide. A completed test vehicle is illustrated in Figure 3.

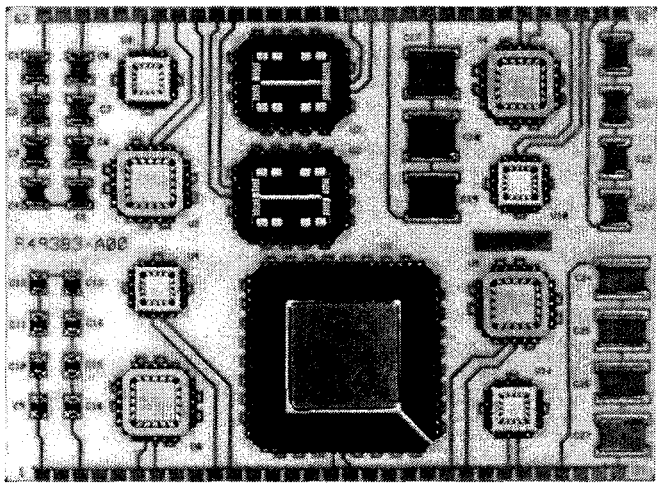

Figure 3. Hybrid microcircuit test vehicle with components soldered in place with Sn-Pb alloy.

The circuit design has a daisy-chained configuration to permit the measurement of electrical continuity during testing. A dielectric was deposited around the metallized features. The test components consist of a variety of dummy chip capacitors (0805, 1810, 1210, 1825 and 2225). The chip capacitors used in this study have 100% Sn terminations. The LCCC's have Au castellations with 16, 20, 32 or 68 input/outputs (I/O's) and a 50 mil pitch.

The Sn-Ag-Bi and Sn-Ag-Bi-Au alloys were fabricated as ingots at Sandia. They were then processed into a powder 30-70 microns in diameter at the Materials Preparation Center at Iowa State University in Ames, Iowa. The powder was mixed with an RMA-based flux vehicle to form a paste with a metals content of 90% (wt %). The reflow soldering operation used in this study involves screen printing the solder paste on to the unpopulated test substrate with an 0.008" thick stencil. The components are then placed on the paste. The adhesive properties of the paste holds the components down while the board is heated to a temperature above the melting point of the given solder alloy. The test vehicles were then processed through a

tabletop solder reflow machine. The unit has four conduction heat zones; all of which were optimized for each solder alloy. The heat zones were inerted with technical grade nitrogen, flowing at a rate of 30 SCFH. A sweeper bar moved the part across the heat zones at a pre-determined speed. A time/temperature profile for complete reflow for each assembly and solder paste combination was obtained. The target parameters for this test vehicle that were used included: 1) a 1.5 to 2 min. preheat, 2) a one minute period above reflow temperature and, 3) a peak temperature 20 to 30°C above the melting point of the particular alloy to assure adequate solder reflow.

RESULTS AND DISCUSSION

After test vehicle assembly, but prior to mechanical testing, a comprehensive defect analysis was conducted under a stereo microscope to assess joint geometry, bridges, voids and component misalignment. In addition, solderability of bonding pads, formation of solder balls and thermal damage to the board were assessed. The three lead-free alloys were compared to the performance of Sn-Pb solder.

The populated boards exhibited a variety of minor defects. In particular, the first set of boards printed with each of the four alloys showed limited solder rise up the bare Au castellations on the LCCC's (Fig 4a). It ranged from approximately a 30% rise on the 16 I/O to 85% on the 20 I/O LCCC. However, more solder rose up the castellations on the larger package, irrespective of position. All four sides of the LCCC showed consistent behavior in this regard. The Sn-Pb exhibited the best wetting, while the Sn-Ag-Bi was the poorest. None exhibited 100% rise and the joints were very lean. This was not the case with the chip capacitors. All exhibited good wetting. After this initial observation, all subsequent LCCC's were pre-tinned with the appropriate alloy prior to assembly. Optical images of the Sn-Ag alloy are shown in Fig. 4b, which illustrates the effects of pre-tinning on the shape of the solder fillets. All LCCC's showed much improved solder rise after pre-tinning. This was the case for all of the alloys, but the improvement was most dramatic for the Sn-Ag-Bi.

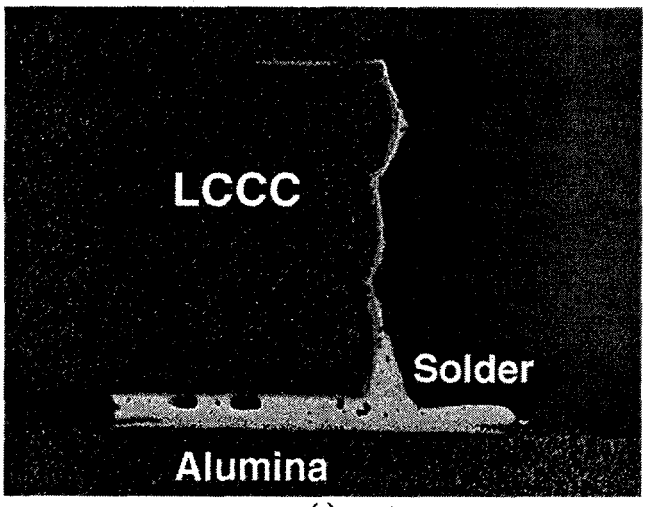

(a)

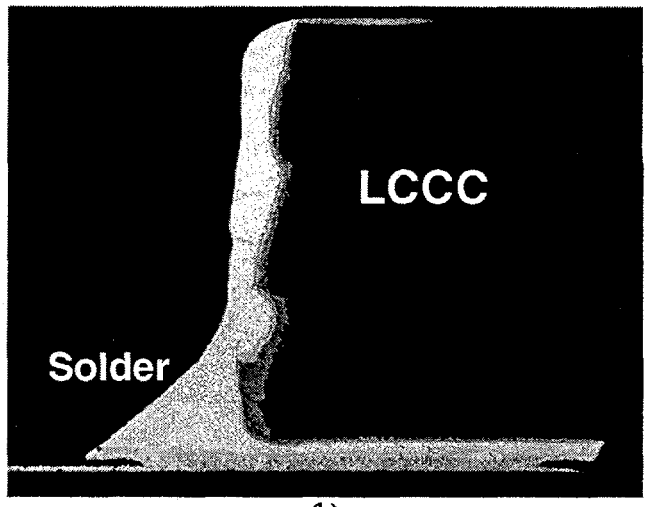

(b)

Fig. 4. Optical images of Sn-Ag solder fillet on 20 I/O LCCC (a) before pre-tinning and (b) after pre-tinning.

The next step in the evaluation was to assess the effect of solid-state aging on the intermetallic layer. Shown in Fig. 5 is a series of photomicrographs illustrating the solder/thick film interface and development of the intermetallic compound as a result of solid state aging at 100°C for the Sn-Pb system. The aging conditions were (a) as fabricated, (b) 1000 hrs., (c) 2000 hrs. and (d) 5000 hrs. The micrograph in Fig. 5b illustrates how the IMC has developed between the thick film and the solder. Concurrently, the printed film is reduced in thickness as the metal component is consumed by the formation of the IMC layer. Photos 5c and 5d show even more extensive growth of the IMC and nearly complete consumption of the thick film as the aging process continues.

In contrast, Figure 6 illustrates how IMC growth progresses in a Pb-free system. The Sn-Ag-Bi alloy is also shown at 100°C for (a) as fabricated condition, (b) 10 hrs., (c) 1000 hrs. and (d) 2000 hrs. While the thick film is still visible in all cases, it is being consumed as the part ages. Note how the microstructure of the solder quickly changes. There has been a coarsening of the Au_xSn_{1-x} particles. Understanding the evolution of these structural changes is very important to the mechanical response of the joint and developing a methodology for predicting service reliability.

The thickness of the IMC layer was modeled by an Arrhenius time and temperature dependence. The graphs in Fig. 7 illustrate how quickly the intermetallic layer grows as time and temperature increase. At 55°C and 70°C, the IMC layer thickness exhibited no significant increase over the aging time. However, at the higher temperatures, 100°C, 135°C and 170°C, the IMC layer thickness increased much more quickly. Note how the graph levels off soon into the aging process at 170°C. This shows that the thickness of the IMC layer has ceased due to complete consumption of the thick film layer.

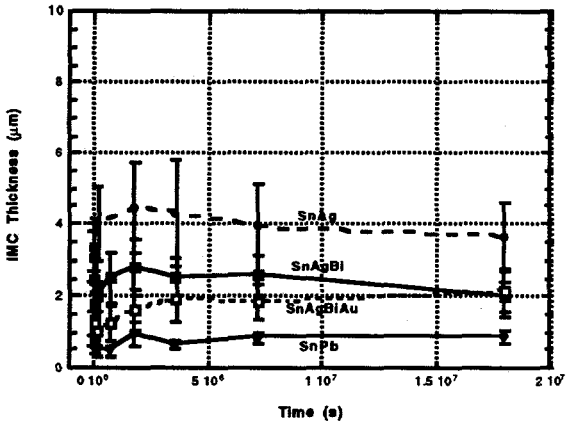

(a) 70°C

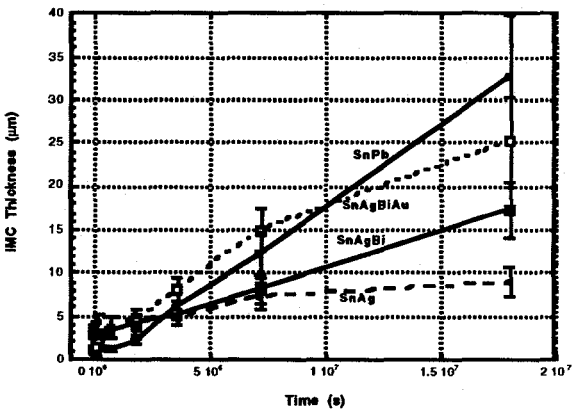

(b) 100°C

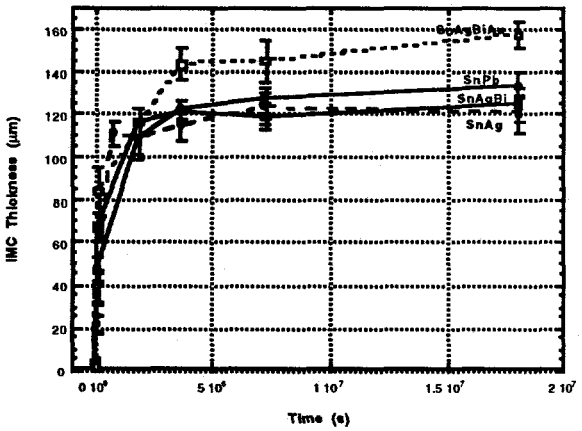

(c) 170°C

Figure 7. IMC layer development for each of the alloys aged at (a) 70°C, (b) 100°C and (c) 170 °C.

Mechanical testing was then performed on representative solder joints. The boards were laser sectioned without damage to any joints. The board segments were introduced into a loading frame with a ram attached to the cross head member of the load frame. At a crosshead speed of 10 mm/min., the ram was used to push the component from the board. Once again, the maximum recorded load, plus or minus one standard deviation, was used to designate the strength of the joint. Four tests were run per sample category. The mechanical test data for the chip capacitors with each alloy is illustrated in Figure 8a. The data shows that the joint strengths of each of the chip capacitors are similar to that obtained with eutectic Sn-Pb. In the case of the 1810 chip capacitor, the joint strength of the Sn-Pb alloy was 28.2 ± 11.3 lbs. while the Sn-Ag-Bi-Au measured 34.0 ± 5.0 lbs. The Sn-Ag-Bi solder had slightly lower joint strengths than Sn-Pb, but those differences were very small. For example, the Sn-Pb measured 89.7 ± 1.7 lbs. for the 1825 chip capacitor while the Sn-Ag-Bi measured 70.4 ± 5.6 lbs. The LCCC test data is shown separately in Fig. 8b, since the pre-tinning of these components had an effect on the mechanical properties. Although there was a slight increase in the joint strength of the Sn-Pb solder after pre-tinning, the Pb-free LCCC's showed a dramatic increase in joint strength after pre-tinning. The Sn-Pb joint strengths of the LCCC 20 rose from 172.4 ± 12.8 lbs. before pre-tinning to 204.4 ± 16.0 lbs. after pre-tinning. However, the strengths of the Pb-free alloys almost doubled from 53.2 ± 2.0 lbs. on the LCCC 16 to 95.6 ± 0.8 lbs. after pre-tinning. Similar results were obtained for the Sn-Ag-Bi-Au also showing an increase on the LCCC 20 from 110.8 ± 20.0 to 225.6 ± 5.2 lbs. after pre-tinning of the components. These differences in mechanical strengths show how important joint geometry and shape of the solder fillet is to the overall reliability of a solder joint.

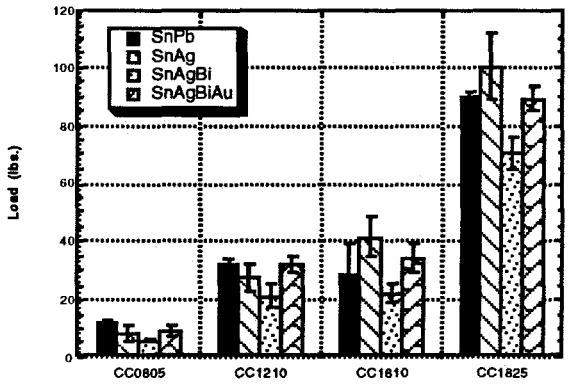

(a)

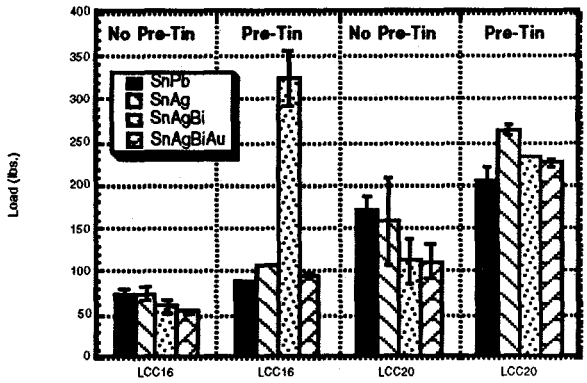

(b)

Figure 8. Mechanical test data for components soldered to test vehicle with each of the four alloys. Chip capacitor data is shown in (a) while LCCC data is shown in (b). Mechanical strength of LCCC joints increased slightly after the components were pre-tinned.

CONCLUSIONS

Solid state aging and mechanical strength of joints have been evaluated on prototype surface mount circuit boards. Intermetallic compound layer formation was examined between the thick film composition Au76-Pt21-Pd3 over Al_2O_3 and the solders: Sn96.5-Ag3.5 (wt %), Sn91.84-Ag3.33-Bi4.83, Sn86.85-Ag3.15-Bi5.00-Au5.00 and Sn63-Pb37 (control). The IMC layer growth kinetics differed between the various solders, resulting in thickness trends that were time and temperature dependent. Although Sn-Pb solder consistently yielded the best wetting and joint formation, the other Pb-free solders offer potential for component attachment in surface mount technology. The joint strengths of the Pb-free alloys are very comparable to those of eutectic Sn-Pb solder. The shear data of the ring-and-plug test specimens were higher for the Pb-free alloys than for eutectic Sn-Pb.

ACKNOWLEDGMENTS

The authors would like to acknowledge the efforts of James Gonzales for his help with the screen printing of the solder pastes; Charlie Carter and Alice Kilgo for metallographic sample preparation and optical micrographs and Barry Ritchie for his scanning electron microscopy efforts. The manuscript was reviewed by Mike Hosking.

REFERENCES

[1] C. Lea, "A Scientific Guide to Surface Mount Technology", Electrochemical Publications Limited, Scotland, pp. 1, 2, 1988.

[2] Paul Vianco, Jerry Rejent, Iris Artaki, Urmi Ray, Donald Finley, Anna Jackson, "Compatibility of Lead-Free Solders with Lead Containing Surface Finishes as a Reliability Issue in Electronic Assemblies", 46th Electronic Components & Technology Conference, p.1172-1173, 1996.

[3] Norbert Socolowski, "Lead-Free Alloys and Limitations for Surface Mount Assembly", Surface Mount International Proceedings (SMI, '95), p.477, 1995.

[4] Ning-Cheng Lee, James A. Slattery, John R. Sovinsky, Iris Artaki, Paul T. Vianco, "A Novel Lead-Free Solder Replacement", Surface Mount International Proceedings (SMI, '94), p. 465, 1994.

[5] P. Holmes and R. Loasby, "Handbook of Thick Film Technology", Electrochemical Publications, Ltd., Ayr, Scotland, UK, 1976, p. 97-108.

[6] Paul T. Vianco, John J. Stephens, Jerome A. Rejent, "Intermetallic Compound Layer Development During the Solid State Thermal Aging of 63Sn-37Pb Solder/Au-Pt-Pd Thick Film Couples", IEEE Transactions on Components, Packaging and Manufacturing Technology, p. 479-485, 1997.

[7] D. R. Frear and P. T. Vianco, "Intermetallic Growth and Mechanical Behavior of Low and High Melting Temperature Solder Alloys", Metallurgical and Materials Transactions, Vol. 25A, p. 1509, 1994.

[8] Mathew Schaefer, Werner Laub, Janet M. Sabee, Raymond A. Fournelle, "A Numerical Method for Predicting Intermetallic Layer Thickness Developed During the Formation of Solder Joints", Jounal of Electronic Materials, Vol. 25, No. 6, p. 992, 1996.

[9] F. M. Hosking, P. T. Vianco, J. A. Rejent, C. L. Hernandez, "Environmentally Compatible Solder Materials for Thick Film Hybrid Assemblies", ASME International Intersociety Electronic & Photonic Packaging Conference Proceedings (INTERPACK '97), p. 1364, 1997.

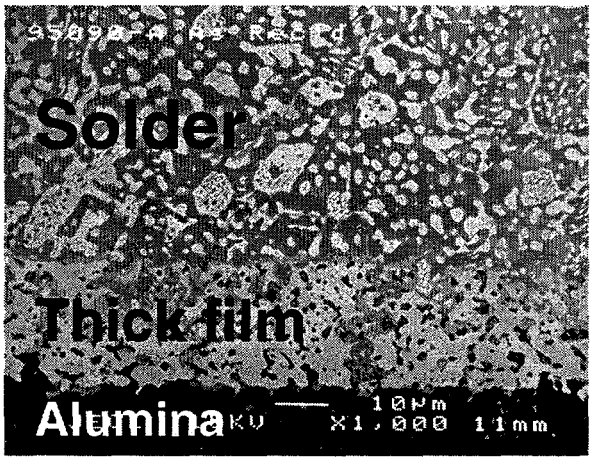

(a) "as fabricated"

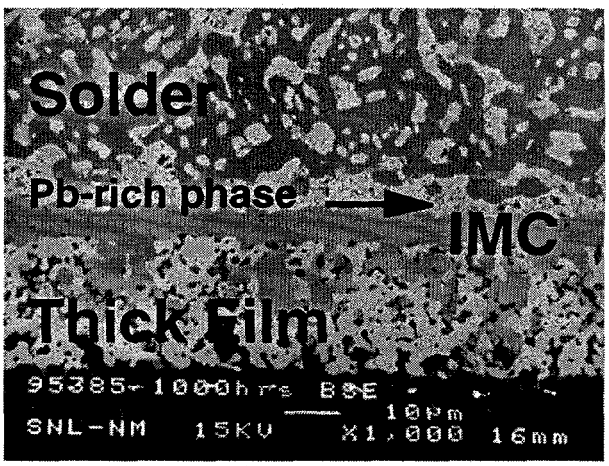

(b) 1000 hrs.

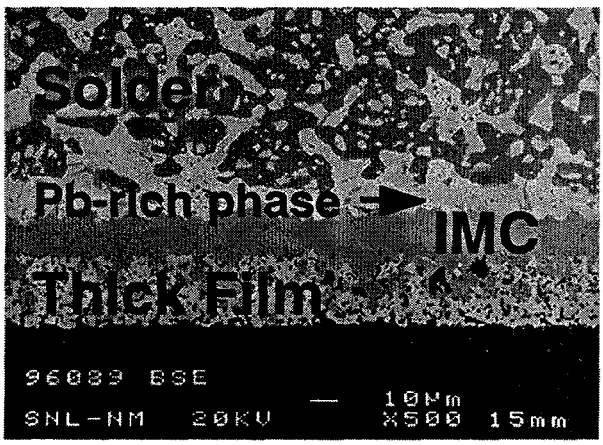

(c) 2000 hrs.

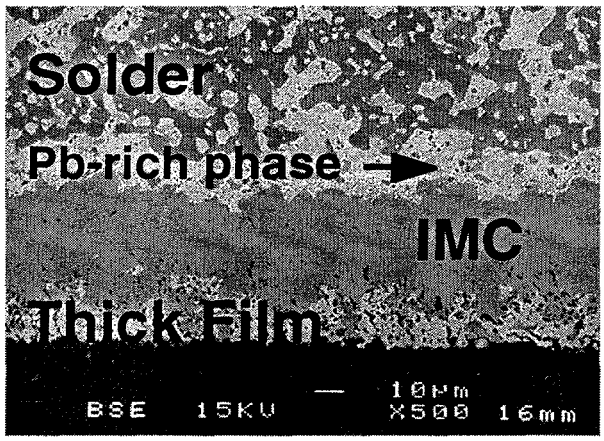

(d) 5000 hrs.

Figure 5. SEM/backscattered emission micrographs of the interface between the Au-Pt-Pd thick film and Sn-Pb solder showing the development of the intermetallic compound layer as a result of solid state aging at 100°C: (a) as-fabricated, (b) 1000 hrs., (c) 2000 hrs. and (d) 5000 hrs.

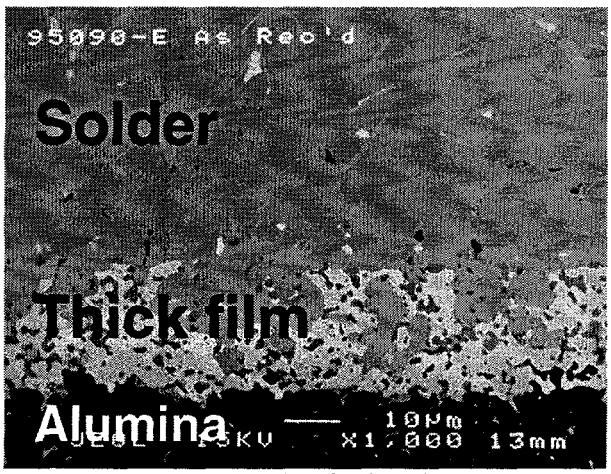

(a) as fabricated

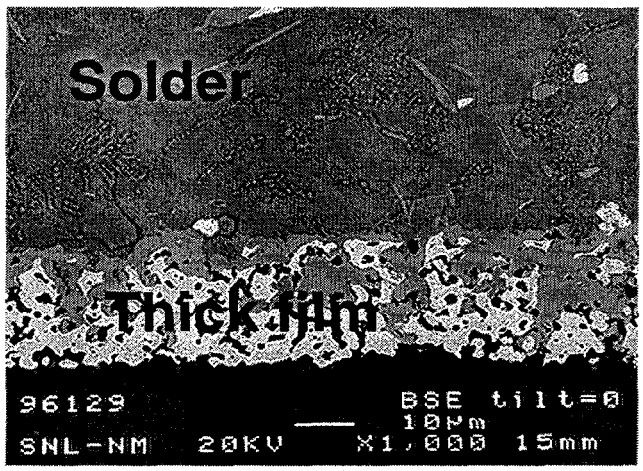

(b) 25 hrs.

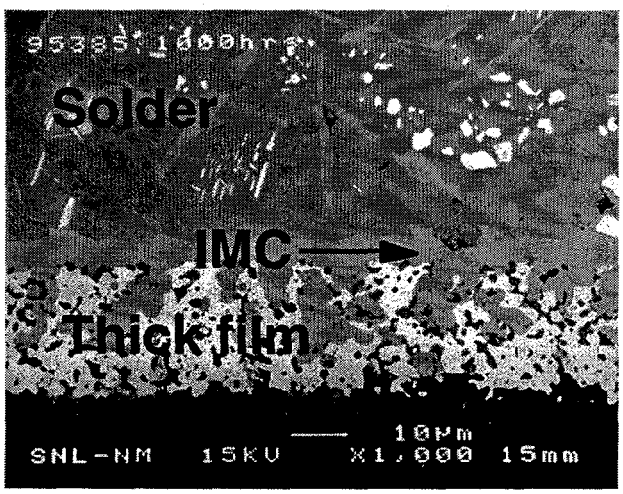

(c) 1000 hrs.

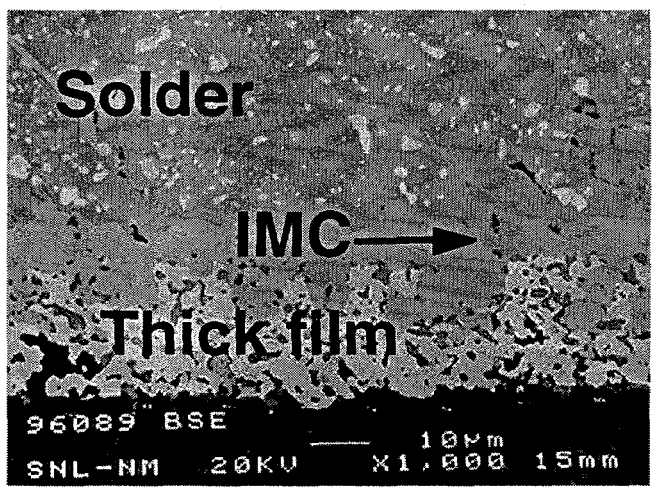

(d) 2000 hrs.

Figure 6. SEM/backscattered emission micrographs of the interface between the Au-Pt-Pd thick film and Sn-Ag-Bi solder showing the development of intermetallic compound layer as a result of solid state aging at 100°C: (a) as-fabricated, (b) 25 hrs., (c) 1000 hrs. and (d) 2000 hrs.